Dynamics of modern epidemics

Dirk Brockmann, Lars Hufnagel, and Theo Geisel

11.1 Summary

The application of mathematical modelling to the spread of epidemics has a long history and was initiated by Daniel Bernoulli's work on the effect of cow-pox inoculation on the spread of smallpox in 1760 (Bernoulli 1760). While most studies concentrate on the temporal development of diseases and epidemics, their geographical spread is less well understood. The key question and difficulty is how to include spatial heterogeneities and to quantify the dispersal of individuals (Keeling *et al*. 2001; Smith *et al*. 2002; Keeling *et al*. 2003; Lipsitch *et al*. 2003). In a well established class of models spatial dispersal is accounted for by ordinary diffusion (Murray 1993). This approach admits a description in terms of reaction-diffusion equations which generically exhibit epidemic wavefronts propagating at constant speeds. These wave fronts were observed for instance in the geo-temporal spread of the Black Death in Europe from 1347–50 (Langer 1964; Noble 1974; Mollison 1991; Grenfell *et al*. 2001). However, today's volume, speed, and non-locality of human travel (Fig. 11.1) and the rapid worldwide spread of severe acute respiratory syndrome (SARS) (Fig. 11.2) demonstrate that modern epidemics cannot be accounted for by local diffusion models, which are only applicable as long as the mean distance travelled by individuals is small compared to the geographical scope of the model.

In this chapter, we focus on mechanisms of the worldwide spread of infectious diseases in a modern world in which humans travel on all scales. We introduce a probabilistic model which accounts for the worldwide spread of infectious diseases on the global aviation network. The analysis indicates that a forecast of the geographical spread of an epidemic is indeed possible, provided that local dynamical parameters of the disease such as the reproduction number are known. The model consists of local stochastic infection dynamics and stochastic transport of individuals on the worldwide aviation network which takes into account the national and international civil aviation traffic. In broad terms, our simulations of the SARS outbreak are in good agreement with published case reports. We propose that our model can be employed to predict the worldwide spread of future infectious diseases and to identify endangered regions in advance. Based on the connectivity of the aviation network we evaluate the performance of different control strategies and show that a quick and focused reaction is essential to inhibit the global spread of epidemics.

11.2 Local infection dynamics

Mathematical models for the description of epidemic outbreaks are rather abundant. Depending on their purpose they differ in their degree of detail (Anderson and May 1991). Some models are designed to reproduce the dynamics of a specific disease with as much accuracy as possible, whereas other models are conceived to reveal the central and general mechanisms underlying an epidemic outbreak. Almost all models share the goal of accounting for the time evolution of the number of infected individuals $I(t)$ in a population of size N. One of the most successful models is the *SIR*-scheme, in which a population of size N is classified into susceptibles (S), infecteds (I), and recovered/removed (R) individuals. The quantities
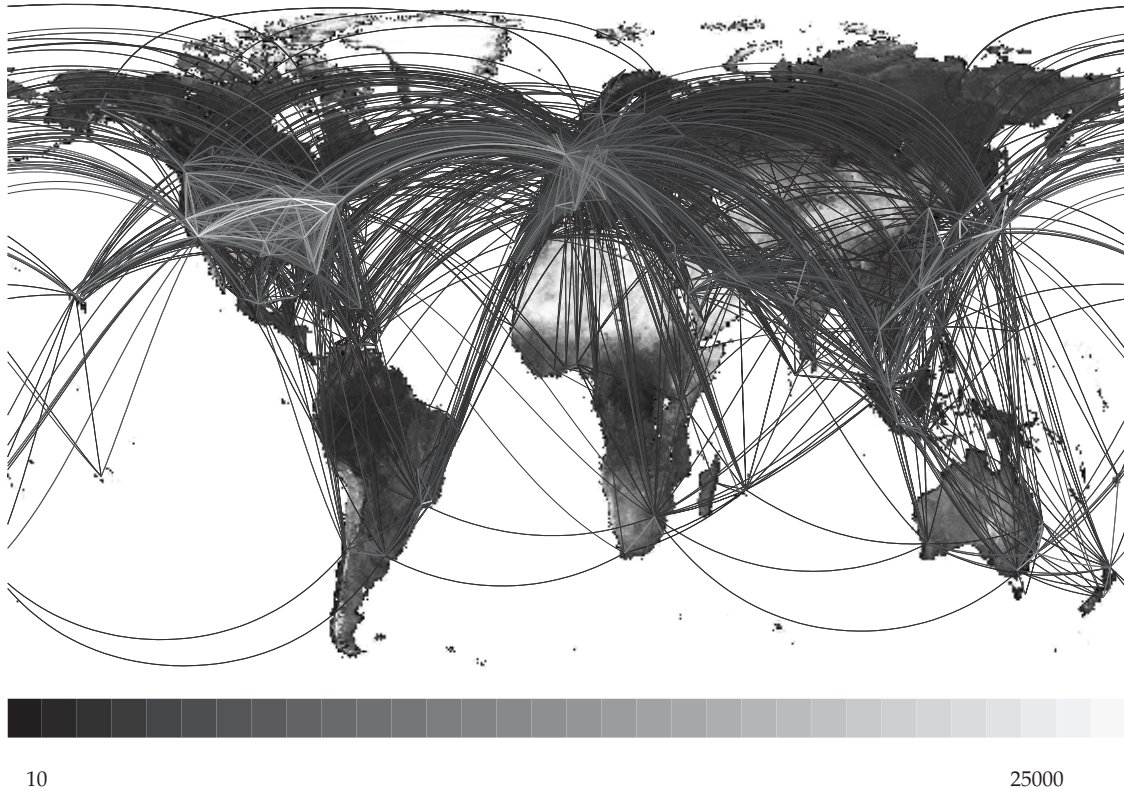
Figure 11.1 Global aviation network. A geographical representation of the civil aviation traffic among the 500 largest international airports in over 100 different countries is shown. Each line represents a direct connection between airports. The gray scale of the connections encodes the number of passengers per day (see lower gray code) travelling between two airports. The network accounts for more than 95% of the international civil aviation traffic.

S, I and R are dynamic, while the total number of individuals is conserved, that is,

$$S(t) + I(t) + R(t) = N. \tag{11.1}$$

The infection dynamics are given by

$$\frac{\mathrm{d}S}{\mathrm{d}t} = -\frac{\alpha}{N}SI, \qquad \frac{\mathrm{d}I}{\mathrm{d}t} = \frac{\alpha}{N}SI - \beta I, \tag{11.2}$$

in which it is assumed that the rate of change of susceptibles and infected is proportional to the transmission rate α as well as the concentration of infecteds and susceptibles, respectively. The second term in the second equation takes into account that infecteds recover or are effectively removed from the population at a rate β. The time course of recovereds $R(t)$ is given by the conservation law (11.1). The initial conditions $I(t_0)$ and $S(t_0)$ along with the parameters N, α, and β determine the evolution of the system. The parameter $R_0 = \alpha/\beta$ is known as the reproduction number of the epidemic, that is, the average number of infections transmitted by an infected individual during the period $\tau = \beta^{-1}$ which is the time an infected individual is infectious. A requirement for an epidemic to occur ($\mathrm{d}I/\mathrm{d}t(t_0) > 0$) is a reproduction number greater than unity and an initial relative number of susceptibles $S(t_0)/N > R_0^{-1}$ (assuming that $R(t_0) = 0$). The peak number of infected individuals $I_{\max}$ is given by $I_{\max}/N = 1 - (1 + \ln\ R_0)/R_0 < 1$. Dividing by the size of the population N and rescaling time as $t \to \beta t$ the dynamics (11.2) can be expressed in terms of the relative concentrations $s = S/N$ and $j = I/N$ of
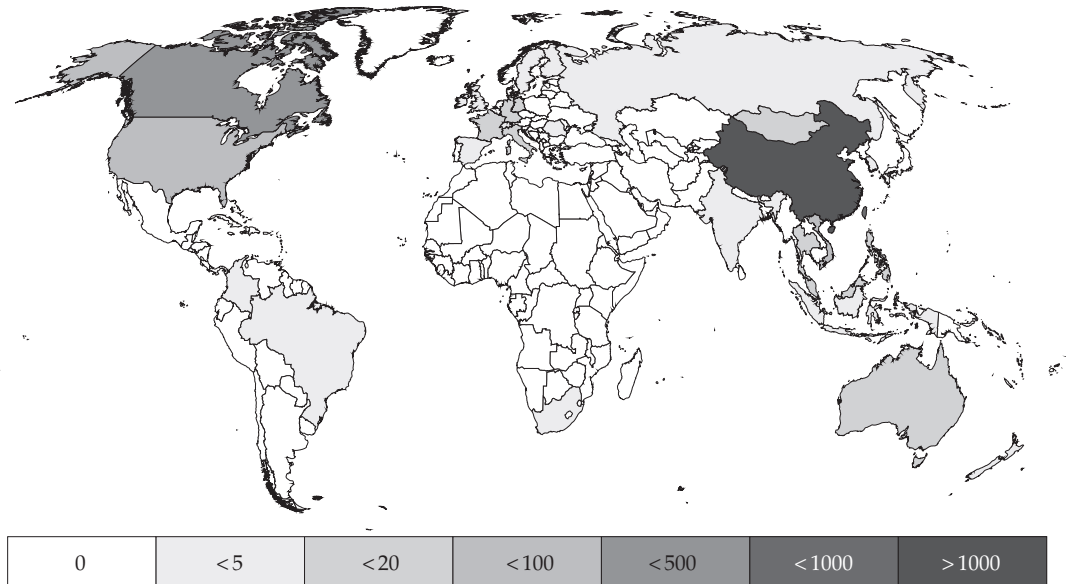
Figure 11.2 Geographical representation of the global spread of probable SARS cases on 30 May 2003 as reported by the World Health Organization (WHO) and the Centers for Disease Control and Prevention (CDC) (Centers for Desease Control and Prevention 2003). The first cases of SARS emerged approximately 5 months earlier in mid November 2002 in Guangdong Province, China.

susceptibles and infecteds respectively and the reproduction number R_0,

$$\frac{dS}{dt} = -R_0 sj, \qquad \frac{dj}{dt} = R_0 sj - j. \qquad (11.3)$$

Time in Eqn (11.3) is measured in units of the time β^{-1} an individual remains infected. The sole parameter which remains is the reproduction number R_0, the population size has dropped out. This implies for instance that the dynamics of a population with $N = 100,000$ and an initial number of infected $I(t_0) = 100$ exhibits the same dynamics of $j(t)$ as a population with $N = 10,000$ and $I(t_0) = 10$. However, while in population of $N = 100,000$ an initial number of infected $I(t_0) = 5$ makes sense, the analogous initial number of infecteds $I(t_0) = 0.5$ in the population with $N = 10,000$ makes no sense, since there is no such thing as half an infected person. The quantization of individuals is not accounted for by the model defined by Eqn (11.3). In short, ignoring stochastic effects in finite populations, as we have done above, can be a crucial drawback. We

will see in the next section that quantization effects are important for they imply a strong impact of the fluctuations of the system which are neglected by the simple deterministic model above.

11.3 The impact of chance

The above SIR model has been able to account for experimental data in a number of cases indicating that Eqn (11.3) incorporate the underlying mechanism of transmission and recovery dynamics. However, transmission of and recovery from an infection are intrinsically stochastic processes and the deterministic SIR model does not account for chance fluctuations. These fluctuations are particularly important at the beginning of an epidemic when the number of infecteds is very small. The understanding of this initial phase of an epidemic is crucial for making any kind of prediction concerning the probability of outbreak in a population and the typical time lag for a given rate of immigration of infecteds.

In order to describe the initial phase, one needs to cast the dynamics of transmission and recovery into a probabilistic model. We begin with the reaction scheme given by

$$S + I \xrightarrow{\alpha} 2I, \quad I \xrightarrow{\beta} \emptyset. \tag{11.4}$$

The first reaction reflects the fact that an encounter of an infected individual with a susceptible results in two infecteds at a probability rate α, the second indicates that infecteds are removed (recover) at a rate β and effectively disappear from the population. The quantity of interest is the probability $p(S, I; t)$ of finding a number S of susceptibles and I infecteds in a population of size N at time t. Assuming that the process is Markovian on the relevant timescales, the dynamics of this probability are governed by the master equation

$$\partial_t p(S,I;t) = \frac{\alpha}{N}(S+1)(I-1)p(S+1,I-1;t)$$
$$+ \beta(I+1)p(S,I+1;t)$$
$$- \left(\frac{\alpha}{N}SI - \beta I\right)p(S,I;t). \tag{11.5}$$

The first term corresponds to the stochastic event $(S+1, I-1) \rightarrow (S, I)$, that is a susceptible is infected, the second term to the event $(S, I+1) \rightarrow (S, I)$, that is an infected recovers from the disease, the third term to the events $(S, I) \rightarrow (S - 1, I + 1)$ and $(S, I) \rightarrow (S, I-1)$.

The relation of the probabilistic master Eqn (11.5) to the deterministic SIR-model (11.3) is not obvious as the set of equations (11.3) describe the evolution of the quantities $s(t)$ and $j(t)$ whereas the master equation (11.5) describes the evolution of the probability of finding $S(t)$ susceptibles and $I(t)$ infecteds at time t.

However, this gap can be bridged by investigating the master equation in the limit of a large but finite population, that is, $N \gg 1$. In this limit one can approximate the master equation by a Fokker–Planck equation by means of an expansion in terms of conditional moments (Kramers-Moyal expansion, Gardiner 1985) which is a standard technique in the theory of stochastic processes. This procedure yields the associated description in terms of stochastic Langevin equations

$$ds = -R_0 sj\,dt + \frac{1}{\sqrt{N}}\sqrt{R_0 sj}\,dW_1(t) \tag{11.6}$$

$$dj = R_0 sj\,dt - j\,dt - \frac{1}{\sqrt{N}}\sqrt{R_0 sj}\,dW_1(t)$$
$$+ \frac{1}{\sqrt{N}}\sqrt{j}\,dW_2(t) \tag{11.7}$$

having rescaled time as $t \rightarrow \beta t$. Here, the independent Gaussian white noise forces $dW_1(t)$ and $dW_2(t)$ (with $\langle dW_i(t)\rangle = 0$ and $\langle dW_i(t)^2\rangle = dt$) reflect the fluctuations of transmission and recovery, respectively. Note that the magnitude of the fluctuations are $\propto 1/\sqrt{N}$ and disappear in the limit $N \rightarrow \infty$. In this limit the dynamics (11.6) and (11.7) reduce to the deterministic SIR-model as defined by (11.3) above. However, for large but finite N a crucial difference to Eqn (11.3) is apparent: (1) eqns (11.6) and (11.7) contain fluctuating forces, (2) the population size is a parameter of the system.

For very large, but finite N one expects from Eqns (11.6) and (11.7) that the impact of the noise is small. However, a careful analysis shows that even in this regime, the noise plays a prominent role in the initial phase of an epidemic outbreak and cannot be neglected. Qualitatively this can be understood as follows: assume that initially nearly the entire population is susceptible, that is, $s \approx 1$ and that the disease has an $R_0 > 1$. According to Eqns (11.6) and (11.7) the expected change of the relative number of infecteds $\langle \Delta j\rangle$ in a short time interval Δt is approximately given by

$$\langle \Delta j\rangle \approx (R_0 - 1)j_0 \Delta t, \tag{11.8}$$

where j_0 is the initial relative concentration of infecteds. The relative typical variability of the change Δj relative to the expected change is given by the standard deviation divided by the mean which is of the order of $1/N j_0$, that is,
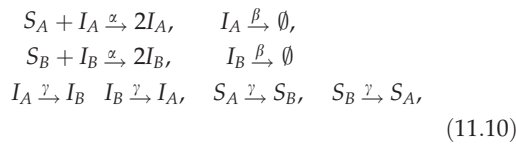
$$\frac{\sqrt{\langle(\Delta j)^2\rangle}}{\langle \Delta j\rangle} \approx \frac{1}{N j_0}. \tag{11.9}$$

For arbitrary initial values of j_0 this quotient is a small number. However, in epidemics during the initial phase j_0 is of the order of $1/N$ which implies

a variability of order unity. It is important to note that $j = 0$ is an absorbing boundary of the system because if at some point no infecteds are present no epidemic outbreak can occur. Consequently, whether or not an outbreak occurs is a matter of chance. Since any arbitrarily small initial condition $j_0 > 0$ in the deterministic SIR model implies an exponential increase of $j(t)$, it is clear that Eqns (11.3) are of no use in modelling the typical scenario one is confronted with during the initial phase of an epidemic. In the next section we exemplify this reasoning in a system of two coupled populations.

11.4 Interacting populations

Consider the system of two confined populations which exchange individuals as depicted in Fig. 11.3. In each population the dynamics of an epidemic is governed by the simple reaction scheme (11.4). For simplicity we assume that both populations have the same size, that is, $N_A = N_B = N$. In addition to disease transmission and recovery, individuals may traverse from one population to the other at a transition rate γ. Schematically, the entire dynamics is given by

$$S_A + I_A \xrightarrow{\alpha} 2I_A, \qquad I_A \xrightarrow{\beta} \emptyset,$$
$$S_B + I_B \xrightarrow{\alpha} 2I_B, \qquad I_B \xrightarrow{\beta} \emptyset$$
$$I_A \xrightarrow{\gamma} I_B \quad I_B \xrightarrow{\gamma} I_A, \quad S_A \xrightarrow{\gamma} S_B, \quad S_B \xrightarrow{\gamma} S_A,$$

$$(11.10)$$

where the indices label the two distinct populations. The state of the system is given by the probability $p(S_1, I_1, S_2, I_2; t)$ of finding a combination of susceptibles and infecteds in both populations. Along the same lines as presented in the previous section one can construct a master equation for this probability, investigate the limit of large N, and obtain a Fokker–Planck equation in the diffusion limit. Now assume that initially a small number of infected I_0 is introduced to population A without any infecteds contained in B. For a sufficiently high number of infecteds in A an epidemic occurs. For $\gamma > 0$ infecteds are introduced to B and a subsequent outbreak may occur in B after a time lag T. Without noise, that is, in the idealized case of $N \to \infty$ and thus the deterministic SIR-model, any arbitrarily small I_0 triggers two successive outbreaks. This is quite
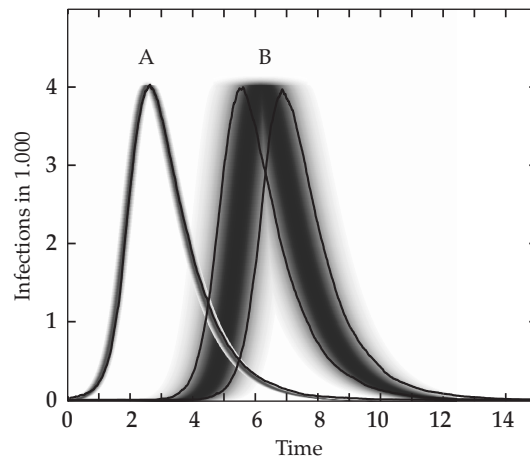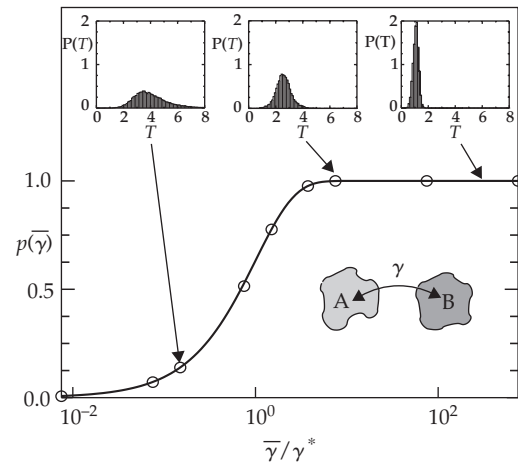

Figure 11.3 Two confined populations with exchange of individuals. In each population the dynamics is governed by the SIR-reaction scheme. Individuals transit from one population to the other at a rate γ. Parameters are $N_A = N_B = 10{,}000$, $R_0 = 4$ and an initial number of infecteds $I_0 = 20$ in population A Left: The probability $p(\gamma)$ of an outbreak occurring in population B as a function of transition rate γ. The insets depict histograms of the time lag T between the outbreaks in A and B for those realization for which an outbreak occurs in B. The circles are results of the simulations of 100,000 realizations, the solid curve is the analytic result of Eqn (11.11) Right: The left black curve represents the time course of $I_A(t)$ of the number if infecteds in population A. The shading reflects the variability of an ensemble of over 100,000 realizations of the process. The trajectories on the right correspond to $I_B(t)$. Two representative realizations are superimposed in black.

different when quantized populations and thus fluctuations are taken into account.

Figure 11.3 depicts the results of simulations for two populations with $N = 10{,}000$ and $R_0 = 4$. Various realizations of the time course $I_A(t)$ and

$I_B(t)$ of the epidemic in both populations were computed. The initial number of infecteds in population A was $I_A (t = 0) = I_0 = 20$. The left panel depicts the probability $p(\gamma)$ that the outbreak is followed by an outbreak in population B as a function of the transition rate γ. For large enough rates the probability is nearly unity, since a sufficient number of infecteds is introduced to B. For very low rates γ no infecteds are introduced to B during the time span of the epidemic in A and thus $p(\gamma) \to 0$ as $\gamma \to 0$. For intermediate values of γ the probability $p(\gamma)$ is somewhere in the range $[0,1]$. This means that in this regime one cannot say with certainty whether an epidemic in A is followed by an epidemic in B. This effect is caused by the fluctuations of the system. The function $p(\gamma)$ is given by

$$p(\gamma) = 1 - \exp(-\gamma/\gamma^*), \qquad (11.11)$$

where

$$\gamma^* \approx \left(\frac{R_0 + 1}{R_0 - 1}\right) \frac{1}{2I_{\max}}, \qquad (11.12)$$

is a critical rate which is determined by the parameters N and R_0 of the system and the maximum of infecteds $I_{\max}$ in A. The insets depict histograms of the time lag τ for those realization in which an outbreak occurs in B. Each histogram corresponds to a different transition rate γ. The smaller γ the higher the variability in T. Note that even in a range in which $p(\gamma) \approx 1$ (the right-most of the three insets), the time lag T is still a stochastic quantity with a high degree of variance.

The right panel depicts the infection curves $I_A(t)$ and $I_B(t)$ in both populations. Since $j_A (t = 0) \gg 1/N$ in A, the various realizations of $I_A (t)$ nearly coincide. As expected, the impact of fluctuations is small in population A. This is quite different in population B which exhibits a high variability in the time course of $I_B (t)$. Since initially no infecteds are present in this population, the outbreak relies on the immigration of infected from A. Thus, during the initial phase $j_B (t)$ is of the order of $1/N$, the regime in which fluctuations are important. Note, however, that once $j_B (t) \gg 1/N$ the shape of infection curve is relatively uniform and similar to the one predicted by the deterministic model.

Consequently, the introduction of stochastic exchange of infected individuals leads to a lack of predictability in the time of onset of the initially uninfected population. In summary, the investigation of two coupled populations shows that the deterministic SIR-model fails whenever only one population initially contains infected individuals and a full probabilistic description is required.

11.5 Epidemics on networks

The system of two populations can be generalized to an arbitrary number M of populations in a straightforward manner. For simplicity, we assume that the epidemiological parameters α and β and hence the reproduction number R_0 are identical in all populations. In addition to the transmission and recovery dynamics

$$S_i + I_i \xrightarrow{\alpha} 2I_i, \qquad I_i \xrightarrow{\beta} \emptyset, \quad i = 1, \dots, M, \qquad (11.13)$$

dispersal of individuals is defined by a matrix γ_{ij} of transition rates between populations

$$S_i \xrightarrow{\gamma_{ij}} S_j \qquad I_i \xrightarrow{\gamma_{ij}} I_j, \quad i, j = 1, \dots, N, \qquad (11.14)$$

where $\gamma_{ii} = 0$. Let us assume that the total number of individuals $\mathcal{N} = \sum_i^{\mathcal{M}} \mathcal{N}_i$ is fixed. For a predefined matrix γ_{ij} the relative concentration of individuals $c_i = N_i/\mathcal{N}$ changes over time. The dynamics of $c_i (t)$ can be interpreted as the probability of finding an individual in population i. This quantity is determined by the master equation for dispersal, that is,

$$\partial_t c_i = \sum_j (\gamma_{ij} c_j - \gamma_{ij} c_i). \qquad (11.15)$$

The stationary state $c_i^* i = 1, \dots, M$ is given by

$$\frac{\gamma_{ij}}{\gamma_{ji}} = \frac{c_i^*}{c_j^*} = \frac{N_i^*}{N_j^*}. \qquad (11.16)$$

In a realistic system, it is reasonable to assume stationarity of dispersal, that is, $N_i(t) \approx N_i^*$ and that the exchange rates between populations fulfill (11.16). Generally, for populations of identical size (i.e. $N_i = N$) the above condition implies that $\gamma_{ij} = \gamma_{ji}$ of every pair (i, j) of populations. Note that this

does not imply that all rates are identical, for example, one might have $\gamma_{12} = \gamma_{21}$ and $\gamma_{34} = \gamma_{43}$ but $\gamma_{12} \neq \gamma_{34}$.

Consider a system as depicted in Fig. 11.4. Each population contains N individuals. A central population A is coupled to a set of $M-1$ surrounding populations $B_1, \ldots B_{M-1}$. The exchange rates between the central ($i=0$) and a surrounding population j are the same, that is, $\gamma_{0j} = \gamma_{j0} = \gamma_j$ with $j = 1, \ldots, M-1$. However, the set of rates γ_j can be highly variable.

Assume that initially a number of infecteds I_0 is introduced to the central population A such that an outbreak occurs. Furthermore we assume that there are initially no infecteds in the surrounding populations. The entire set of rates $\{\gamma_j\}_{j=1, \ldots, M-1}$ determines the behaviour in the surrounding populations. If all rates γ_j are identical and very small we expect no infection to occur in the B_j, for large enough γ_j an outbreak will occur in every B_j.
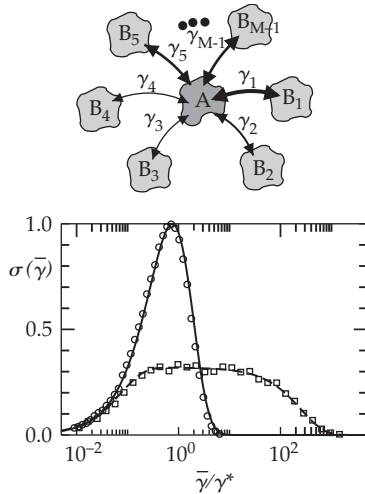

Figure 11.4 Inhomogeneous connections and predictability. Left: A star-like network with a central population A connected to M − 1 populations $B_1, \ldots, B_{M-1}$ with rates $\gamma_1, \ldots, \gamma_{M-1}$. Right: The cumulated variance (Eqn 11.9) for a star network with 32 populations is depicted as a function of the average transmission rate $\bar{\gamma}$. Two cases are exemplified: equal rates (circles) and distributed rates according to Eqn (11.19) with $\gamma_{max}/\gamma_{min} \approx 1000$ (squares). The solid and dashed lines shows the analytical results given by Eqns (11.17) and (11.111), respectively. Parameters are N = 10,000 for all populations, $R_0 = 4$ and an initial number of infecteds $I_0 = 20$ in population A. The numerical values are obtained by calculating the variance of the fluctuations of 100 different realizations of the epidemic outbreak for each $\bar{\gamma}$

In a realistic network, however, transition rates are distributed on many scales and the response of the network to a central outbreak depends on the statistical properties of this distribution. We denote the probability density of rates by $\pi(\gamma)$.

In order to quantify the reaction of the network we introduce for each surrounding population a binary number ξ_j with $j = 1, \ldots, M-1$ which is unity if an outbreak occurs in B_j and zero if it does not. The variability of the entire network is quantified be the cumulative variance per population and we define

$$\sigma \equiv \frac{4}{M-1} \sum_i \mathrm{var}(\xi_i)$$
$$= \int \mathrm{d}(\gamma) d(\gamma) \, (1 - p(\gamma)) \pi(\gamma) \qquad (11.17)$$

as a measure for the uncertainty of the network response where $p(\gamma)$ is the probability of outbreak as defined by (11.12). If, for example, all transition rates are identical and equal to $\bar{\gamma}$ (i.e. $\pi(\gamma) = \delta(\gamma - \bar{\gamma})$) one obtains

$$\sigma(\bar{\gamma}) = 4p(\bar{\gamma})(1 - p(\bar{\gamma})) \qquad (11.18)$$

which is unity for $p(\bar{\gamma}) = \frac{1}{2}$. Comparing with Eqn (11.11) we see that the system with identical transition rates $\gamma_i = \bar{\gamma}$ exhibits the highest degree of unpredictability when the rates are of the order of the critical rate γ^*. The function $\sigma(\bar{\gamma})$ is shown in Fig. 11.4. The assumption of identical transition rates γ_i is never met in real networks of populations. Typically, the transition rates vary considerably between various nodes in a network. Consider for instance the aviation network (Fig. 11.1) where the transport rates vary over many orders of magnitude. The inset depicts a histogram of the flux of individuals from the set of nodes. This indicates that transition rates are distributed on many scales. A high degree of variability in the rates can be accounted for by a probability density

$$\pi(\gamma) = \frac{1}{\log(\gamma_{max}/\gamma_{min})} \frac{1}{\gamma} \quad \gamma_{max} \leq \gamma \leq \gamma_{min}, \qquad (11.19)$$

where the interval $[\gamma_{min}, \gamma_{max}]$ incorporates many orders of magnitude. Inserting into Eqn (11.17)

yields $\sigma(\bar{\gamma})$ for strongly distributed rates. In Fig. 11.4 this function is compared to a system of identical transition rates. Clearly, a high variability in rates drastically changes the degree of predictability. On one hand, for intermediate values of $\gamma \approx \gamma^*$ the predictability is much higher than in the system of identical rates. This is a rather counterintuitive result. Despite the additional randomness in transition rates, the degree of determinism is increased. On the other hand, for large values of the average rate $\bar{\gamma}$ predictability is decreased. We conclude that in order to make a reliable prediction on the epidemic spread on a network, one needs an estimate of the distribution of transition rates, that is, the function $\pi(\gamma)$ and its relation to the critical rate γ^* as determined Eqn (11.12).

11.6 The global spread of SARS—a paradigm

The theoretical investigation presented above lead us to investigate the extent to which a worldwide epidemic can be predicted when the local infection parameters such as the reproduction number R_0 as well as the global dispersal parameters are known. A paradigmatic system is the recent worldwide spread of the Severe Acute Respiratory Syndrome (SARS). Figure 11.2 depicts the geographical representation of the global spreading of probable SARS cases on 30 May 2003 as reported by the World Health Organization (WHO) and Centers for Disease Control and Prevention (CDC). The first cases of SARS emerged in mid November 2002 in Guangdong Province, China (Centers for Desease Control and Prevention 2003). The disease was then carried to Hong Kong on 21 February 2003 and began spreading around the world along international air travel routes, as tourists and the medical doctors who treated the early cases travelled internationally. As the disease moved out of southern China, the first hot zones of SARS were Hong Kong, Singapore, Hanoi (Vietnam), and Toronto (Canada), but soon cases in Taiwan, Thailand, the United States, Europe, and elsewhere were reported.

In order to understand the global spread we combined local infection dynamics appropriate for SARS with the stochastic dispersal of individuals on the civil aviation network as depicted in Fig. 11.1.

11.6.1 Local infection dynamics

For the local infection dynamics we chose an extension of the stochastic SIR model similar to Eqn (11.5). The categories S, I, and R are completed by a category L of latent individuals which have been infected but are not infectious yet themselves, accounting for the latency of the disease. In our simulations individuals remain in the latent or infectious stage for periods drawn from a delay distribution (Donnelly et al. 2003; Riley et al. 2003).

In order to simulate the worldwide spreading of SARS we need to specify the basic reproduction number R_0 and the mean duration of the infectious period $\tau = \beta^{-1}$ of the infection dynamics. For SARS, the distribution of infectious times has been investigated in detail using the case data of the outbreak in Hong Kong (Donnelly et al. 2003) The basic reproduction number and how it changed over time is also known (Lipsitch et al. 2003; Riley et al. 2003).

11.6.2 The aviation network

We collected data which incorporates 95% of the entire civil aviation traffic (IATA 2003). The data comprise flights among the 500 largest international airports in over 100 different countries (AOG 2003). The network considered is depicted in Fig. 11.1. For each pair (i, j) of airports, we checked all flights departing from airport j and arriving at airport i. The amount of passengers carried by a specific flight within one week can be estimated by the size of the aircraft (We used manufacturer capacity information on over 150 different aircraft types) multiplied by the number of days the flight operates in one week. The sum of all flights yields the passengers M_{ij} per week between i and j. The matrix M_{ij} defines the dispersal of individuals on the aviation network. As indicated by the grey code in Fig. 11.1 the matrix elements vary on a number of scales. We computed the total passenger capacity $T_j = \sum_i M_{ij}$ of each airport j per week assuming that flights carry 80% of their capacity and found very good agreement with independently obtained airport capacities.

11.6.3 Modeling dispersal

If we assume that the passenger capacity T_j reflects the need of a catchment area j, this quantity is proportional to the population size N_j at j,

$$N_j \propto T_j. \tag{11.20}$$

Under this assumption the probability w_{ij} that a travelling individual at j is making a transition to i is given by

$$w_{ij} \propto \frac{M_{ij}}{\Sigma_k M_{kj}}. \tag{11.21}$$

Stochastic dispersal of individuals is then governed by the master equation

$$\partial_t P_i = \gamma \sum_j w_{ij} P_j - \gamma P_i, \tag{11.22}$$

where γ is a universal dispersal rate constant which sets the timescale of travelling. The parameter γ can be determined experimentally by measuring the flux of individuals between two arbitrary airports of the network knowing the population sizes of the corresponding catchment areas. The first term in the master equation accounts for the influx of individuals to location i from all other locations j, the second reflects the outflux of individuals from i. In (11.22) the quantity P_i represents any labelled set of individuals. Under the assumption that infecteds I_i and susceptibles S_i exhibit identical dispersal properties, Eqn (11.22) holds for both. We estimated the rate γ by computing the ratio of the number of infected individuals in Hong Kong to the number of infected individuals outside Hong Kong, which is provided by the WHO data.

11.6.4 Results

Figure 11.5(a) depicts a geographical representation of the results of our simulations. Initially, an infected individual was placed in Hong Kong. The basic reproduction number was set to $R_0 = 4.0$ for the first 35 days and subsequently to zero. In a second simulation we chose a time course for $R_0 = 4.0$ for a period of 0–35 days, $R_0 = 1.0$ for days 35–55 and $R_0 = 0.0$ for days 55–∞. Both

simulations lead to similar results. The figure shows the prediction of our model for the spread of SARS 90 days after the initial infection, corresponding to the end of May. We find the results of our simulations to be in remarkable agreement with the worldwide spreading of SARS as reported by the WHO (compare Fig. 11.2): There is an almost one-to-one correspondence between infected countries as predicted by the simulations and the WHO data. Also the numbers of infected individuals in a country agree nicely. This agreement with the reported case seems rather surprising considering that the simulations reflect stochastic single realizations of a stochastic process on a highly coupled network. However, as we have shown in the simple and idealized case investigated in Section 11.5 the high degree of heterogeneity may well increase the predictability and degree of determinism in the system. This is the underlying reason why a forecast of the global spread of an epidemic on the aviation network is indeed feasible.

Figures 11.5(b) and (c) exemplify how our model can be employed to predict endangered regions if the origin of a future epidemic is located quickly. The figures depict simulations of the global spread of SARS 90 days after hypothetical outbreaks in New York and London, respectively. Despite the worldwide spread of the epidemic in each case, the degree of infection of each country differs considerably, which has important consequences for control strategies.

11.7 Control strategies

Vaccination of a fraction of the population reduces the fraction of susceptibles and thus yields a smaller effective reproduction number R_0. If a sufficiently large fraction of the population is vaccinated, R_0 drops below 1 and the epidemic becomes extinct. The global aviation network can be employed to estimate the fraction of the global population that needs to be vaccinated in order to prevent the epidemic from spreading. Figure 11.6 demonstrates that a quick response to an initial outbreak is necessary if global vaccination is to be avoided. The figure depicts the probability $p_n(v)$ of having to vaccinate a fraction v
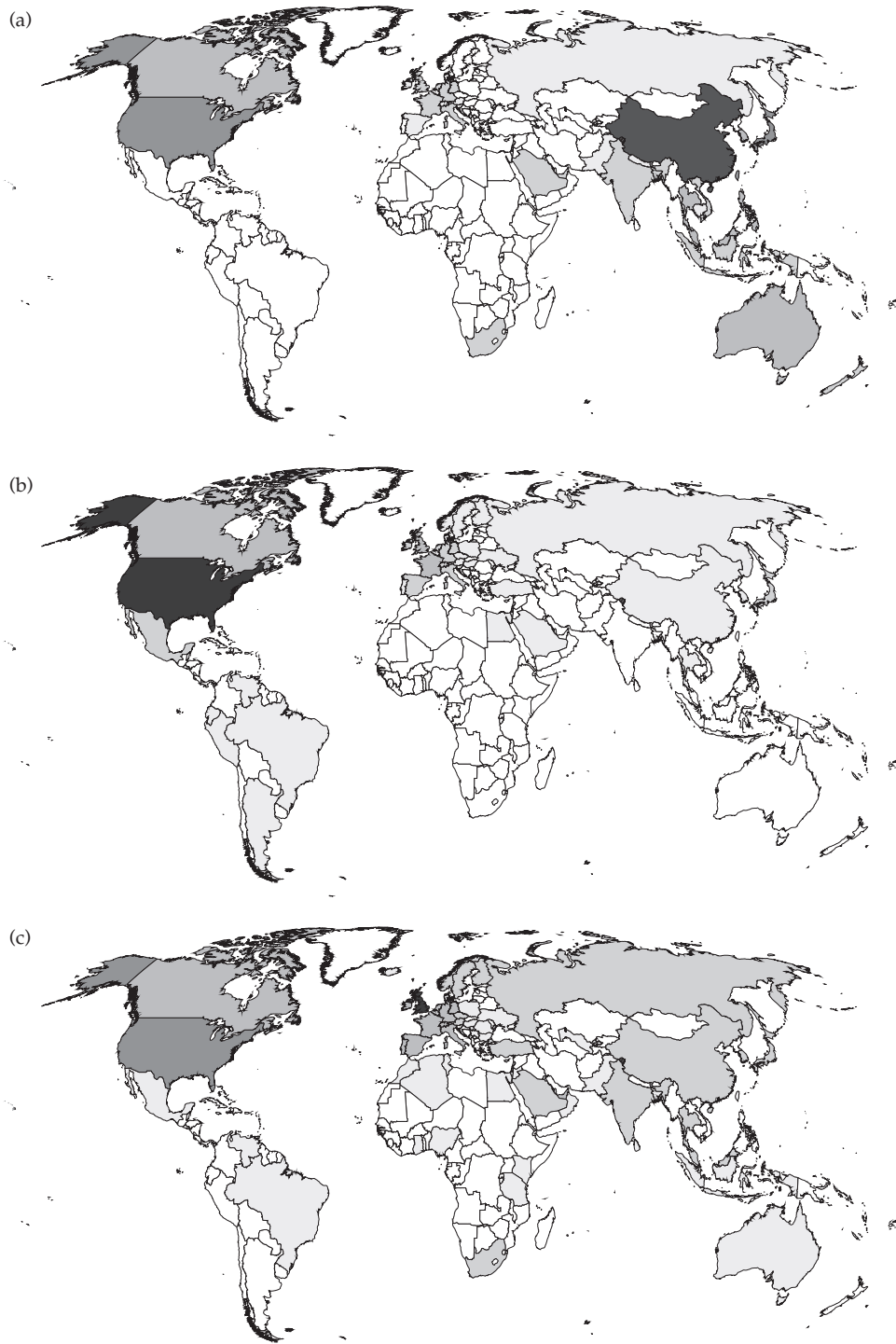
(a)

(b)

(c)

Figure 11.5 Geographical representation of the results of our simulations 90 days after an initial infection in (A) Hong Kong, (B) New York, and (C) London. The same gray code was used as in Fig. 11.2. The simulation in A corresponds to the real SARS infection at the end of May and should be compared to the WHO data shown in Fig. 11.2. Here the worldwide spreading is based on an outbreak starting in Hong Kong in mid February 2003.
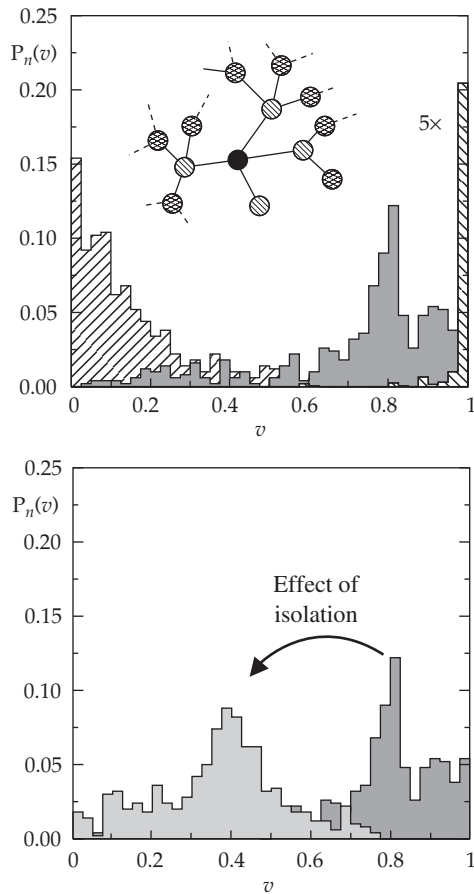
Figure 11.6 Impact and control of epidemics. Left: The probability $p_n(v)$ of having to vaccinate a fraction v of the population in order to prevent the epidemic from spreading, if an initial infected individual is permitted to travel $n=1$ (///), 2 (gray), and 3 (\\\\) times. The probability $p_n(v)$ is estimated by placing the infected individual on a node i (black dot) of the network. The fraction v_n associated with node i is given by the number of susceptibles in the subnetwork defined by the nodes which can be reached by the infected individual after $n=1$, 2, and 3 steps. Histogramming v_i for all nodes i yields an estimate for $p_n(v)$. Right: The quantity $p_2(v)$ exhibits a strong shift to lower values of v when only 2% of the largest cities are isolated after an initial outbreak (light grey) as compared to $p_2(v)$ when no isolation occurs (dark grey).

of the population if an infected individual is randomly placed in one of the cities and permitted to travel $n=1$, 2 or 3 times. For the majority of originating cities the initial spread is regionally confined and thus a quick response to an outbreak requires only a vaccination of a small fraction of the population. However, if the infected individual travels twice, the expected fraction $\langle v \rangle$ of the population which needs to be vaccinated is considerable (74.58%). For $n=3$ global vaccination is necessary.

As a reaction to a new epidemic outbreak, it might be advantageous to impose travel restrictions to inhibit the spread. Here we compare two strategies: (1) the shutdown of individual connections and (2) the isolations of cities. Our simulations show that an isolation of only 2% of the largest cities already drastically reduces $\langle v \rangle$ (with $n=2$) from 74.58% to 37.50% (compare the light-gray and dark grey curves in Figure 11.6). In contrast, a shutdown of the strongest connections in the network is not nearly as effective. In order to obtain a similar reduction of $\langle v \rangle$ the top 27.5% of connections would need to be taken off the network. Thus, our analysis shows that a remarkable success is guaranteed if the largest cities are isolated as a response to an outbreak.

In a globalized world with millions of passengers travelling around the world week by week infectious diseases may spread rapidly around the world. We believe that a detailed analysis of the aviation network represents a cornerstone for the development of efficient quarantine strategies to prevent diseases from spreading. As our model is based on a microscopic description of travelling individuals our approach may be considered a reference point for the development and simulation of control strategies for future epidemics.